

<https://doi.org/10.1038/s43247-024-01245-6>

# Prokaryotic richness and diversity increased during Holocene glacier retreat and onset of an Antarctic Lake

Check for updates

C. Piccini<sup>1</sup>✉, F. Bertoglio<sup>1</sup>, R. Sommaruga<sup>2</sup>, G. Martínez de la Escalera<sup>1</sup>, L. Pérez<sup>3</sup>, L. Bugoni<sup>4</sup>, L. Bergamino<sup>3</sup>, H. Evangelista<sup>5</sup> & F. García-Rodríguez<sup>3,6</sup>

Knowledge about biodiversity changes during transitions from glacial landscape to lake formation is limited to contemporary studies. Here, we combined analyses of lithology, chronology and geochemistry with sedimentary ancient DNA metabarcoding to assess such transition in maritime Antarctica. We inferred three paleoenvironmental stages covering the Holocene glacier retreat process. From 4900 to 3850 years before the present, we found the lowest prokaryotic richness/diversity, with bacterial taxa indicators associated to soil and terrestrial environments. From 3850 to 2650 years before the present, a higher carbon content, higher Carbon/Nitrogen variability, increased species richness/diversity, and prokaryotic taxa indicators of long-term energy starvation were detected. Finally, from 2650 to 1070 years before the present, we inferred the onset of a genuine lacustrine environment holding stable Carbon/Nitrogen ratios and the highest prokaryotic diversity, with known aquatic bacterial taxa. Our study unveils for the first time the evolution from a glacier-covered to a freshwater lake through a millennial scale.

## Main

The reduction and disappearance of glaciers and ice caps affects downstream ecosystems and modify their biodiversity<sup>1</sup>, food webs and fluxes of matter<sup>2</sup>. Recently, a global survey including over 2100 biodiversity studies assessing animal, fungal, vascular plants, and algal taxa demonstrated that richness generally increases (mostly generalist taxa) at lower levels of glacier influence<sup>3</sup>. This suggests that after glacier melting the local biodiversity increases, but the associated long-term environmental effect of specialist taxa depletion exclusively adapted to glacial conditions is still unknown.

Owing to their extremely diverse metabolic capabilities, prokaryotic communities are essential components of aquatic ecosystems. They are involved in fundamental biogeochemical processes, such as organic/inorganic nutrient cycling and energy transfer through the microbial food web<sup>4–6</sup>. Understanding how biogeochemical transformations are mediated by prokaryotes at ecosystem-scale is one of the current challenges of aquatic

microbial ecology<sup>7</sup>. The scarcity of comprehensive data on biodiversity responses to glacier retreat, specifically on microbial diversity, implies that biodiversity of glacial ecotones represents a source of novel scientific information<sup>1</sup>. This lack of information precludes sound conclusions about the effect of ice-sheet loss on ecosystem functioning. Thus, understanding the role of microbial communities and their response to past glacier dynamics is essential to project future changes in ecosystem functioning under the current context of cryosphere evanescence<sup>8</sup>. An approach to reach such predictions is the use of sedimentary ancient DNA (sedaDNA)<sup>9</sup> that helps to reconstruct changes in microbial diversity throughout deglaciation events.

We combined geochemical and sedaDNA metabarcoding analyses to the sedimentary sequence of Lake Profound, the largest proglacial lake of Fildes Peninsula, to assess the transition from glacier-covered area to lake formation. Lake Profound (Antarctic Place-names Committee – APC) is

<sup>1</sup>Instituto de Investigaciones Biológicas Clemente Estable, Centro de Investigación en Ciencias Ambientales, Departamento de Microbiología., Av. Italia 3318, Montevideo 11600, Uruguay. <sup>2</sup>Lake and Glacier Research Group, Department of Ecology, Universität Innsbruck, Technikerstrasse 25, A-6020 Innsbruck, Austria. <sup>3</sup>Universidad de la República, Centro Universitario Regional Este, CURE, Rocha, Uruguay. <sup>4</sup>Universidade Federal do Rio Grande – FURG. Laboratório de Aves Aquáticas e Tartarugas Marinhas, Av. Itália s/n, Campus Carreiros, Rio Grande 96203–900 RS, Brazil. <sup>5</sup>LARAMG/Universidade do Estado do Rio de Janeiro – UERJ, Departamento de Biofísica, Maracanã 0550900 Rio de Janeiro, Brazil. <sup>6</sup>Universidade Federal do Rio Grande, Instituto de Oceanografia, Programa de Pós-Graduação em Oceanologia, Rio Grande – RS, Brazil. ✉e-mail: [cpiccini@iibce.edu.uy](mailto:cpiccini@iibce.edu.uy)

also known as Lake Uruguay, Ozore Glubokoye, and Tiefersee. The Antarctic continent is the largest glacial system on Earth and although both West Antarctic and Antarctic Peninsula are losing ice mass rapidly<sup>10,11</sup>, the continent is still dominated by glaciers and ice masses. Hence, transitional environments are uncommon and constrained to the sub-Antarctic belt. This type of environment is rare because it exhibits a distinct transition from ice-free Antarctic desert to ice sheets with stable mass balance, which are dominated by moraines and many proglacial lakes<sup>12</sup>. Thus, the area selected represents a unique opportunity to study the interactions between glacier frontline and proglacial lakes formation from a paleolimnological viewpoint. Here, the changes in prokaryotic community composition and structure were used as proxies for ecosystem functional changes throughout such long-term landscape to waterscape transformation.

## Lithology and chronology

Sediment obtained in 2019 from Lake Profound (Fig. 1) had two clear sedimentary zones in the core (Fig. 2). Between 75 and 45 cm depth, sediment was characterized by a low moss content, grey hue and pebbles/cobbles, and fine sand without distinct lamination. No other macroscopic biogenic material was observed. Between 45 cm and the surface, it was characterized by abundant presence of moss throughout, light brown color, and a series of silty laminations. The basal section yielded an age of 4910 cal yr BP, corresponding to the middle Holocene (Table 1, Fig. 3). The 55 cm depth yielded an unexpected age of 43,101 cal yr BP. This type of deposit would correspond to transported (not in situ) marine sediments settled during a period of reduced ice extent and reworked as the glacier expanded again<sup>12</sup>. Such a marine material would have been transported from beneath the Collins Ice Cap and deposited initially during a period of reduced ice extent, and then reworked as the glacier expanded over the former seafloor<sup>12</sup>. Thus, this Pleistocene age sample was excluded from the age-depth model (Fig. 3).

Sample from 40 cm yielded an age of 3174 cal yr BP, the 25 cm showed an age of 2615 cal yr BP, at 15 cm the sample showed an age of 2205 cal yr BP and the 3 cm subsurface sample was 1074 cal yr BP. The Bayesian age depth model (Supplementary Data 1) allowed us to infer a low sedimentation, with minimum and maximum values of 0.03 and 0.27 mm yr<sup>-1</sup>, respectively (Table 1, Fig. 3). The age-depth model showed a fairly low linear sedimentation rate throughout. The lowest sedimentation rate was determined from 0 to 15 cm (0.03 and 0.11 mm yr<sup>-1</sup>), while the highest values were recorded from 15 to 40 cm (0.24 and 0.27 mm yr<sup>-1</sup>). Intermediate rate values of 0.13 mm yr<sup>-1</sup> were observed from 40 to 65 cm depth (Table 1, Fig. 3).

## Geochemistry

From the distribution of TOC, TN, C/N, and the element stable isotopes, three core zones were identified at 75% similarity (Fig. 2a). Zone G1, from 70 to 47 cm, showing the lowest TOC and TN concentration and C/N ratios close to 6 (except for the middle section where these values increased). The  $\delta^{13}\text{C}$  ranged between  $-24$  and  $-23$  ‰, but at 55 cm values were close to  $-25$  ‰. The  $\delta^{15}\text{N}$  values were mostly higher than zero within this zone.

Zone G2 spanned from 47 to 26 cm and was characterized by the increase in TOC (Fig. 2a) and a concomitant increase in TN values. Using 80% similarity as cutoff level, this zone was further subdivided into a lower zone G2a and upper zone G2b, where the characteristic feature was the high variability in C/N ratios within the upper subsection from about 5 to ca. 13. The  $\delta^{13}\text{C}$  values decreased from  $-23$  to  $-25$  ‰ and  $\delta^{15}\text{N}$  were always close to  $-1$  ‰. Zone G3, from 26 cm to surface, exhibited the highest TOC and TN values and the striking characteristic was the stabilization of C/N ratios close to 12. The  $\delta^{13}\text{C}$  and  $\delta^{15}\text{N}$  displayed values similar to the previous zone (Fig. 2a).

The SIMMR analysis of isotopic fractional contribution from potential organic matter sources identified a substantial contribution of moss (>40%) > lichens (>35%) > particulate organic matter (POM) (20%) > microbial organic matter (MIC) (10%) (Fig. 2b). The organic matter composition showed no major vertical changes (Fig. 2b, with a steady dominance of moss

and lichens organic matter. The only noticeable change was observed below 55 cm, where the highest moss and POM values were detected.

## Prokaryotic community diversity and composition

A total of 9336 Amplicon Sequence Variants (ASVs) were identified in the database from the sedaDNA samples (Supplementary Data 2). Rarefaction curves based on the observed ASVs richness reached always a plateau (Supplementary Data 3).

Beta diversity calculations to determine whether the differences in prokaryotic community structure over time were due to species replacement ( $\beta_{\text{sim}}$ ) or nestedness ( $\beta_{\text{nes}}$ ) indicated that the former process accounted for most of the change ( $\beta_{\text{sim}} = 0.931$ ,  $\beta_{\text{nes}} = 0.021$ ).

The observed trends using the prokaryotic data matched the geochemical data throughout the core. Using cluster analysis (40% cluster similarity), three different clusters holding distinctive prokaryotic community composition were identified (Permanova analysis,  $p = 0.0001$ ) that were coincident with the geochemistry-based cluster groups (G1 to G3). The identified zones based on their community composition showed differences in the ASVs accounting for 50% of sample abundance and in the indicator ASV (indicator species index) (Fig. 4a, b, Table 2). The non-metric multidimensional scaling (NMDS) analysis revealed clear differences between samples from 67 to 50 cm and with the rest of the sedimentary sequence (Fig. 4c).

Zone B1 (67 to 50 cm) included distinctive ASVs from the genera *Herbaspirillum*, *Sphingomonas*, *Methylobacterium*, and *Moraxella* or *Erhydrobacter*, depending on the classifier. This zone had the lowest ASV richness ( $p$ -value = 0.0064 for B1vs.B2 and  $p$ -value = 0.0005 for B1vs.B3) and Shannon diversity ( $p$ -value = 0.0026 for B1vs.B2 and  $p$ -value = 0.0001 for B1vs.B3) from all three zones, and the highest dominance values (Fig. 4b).

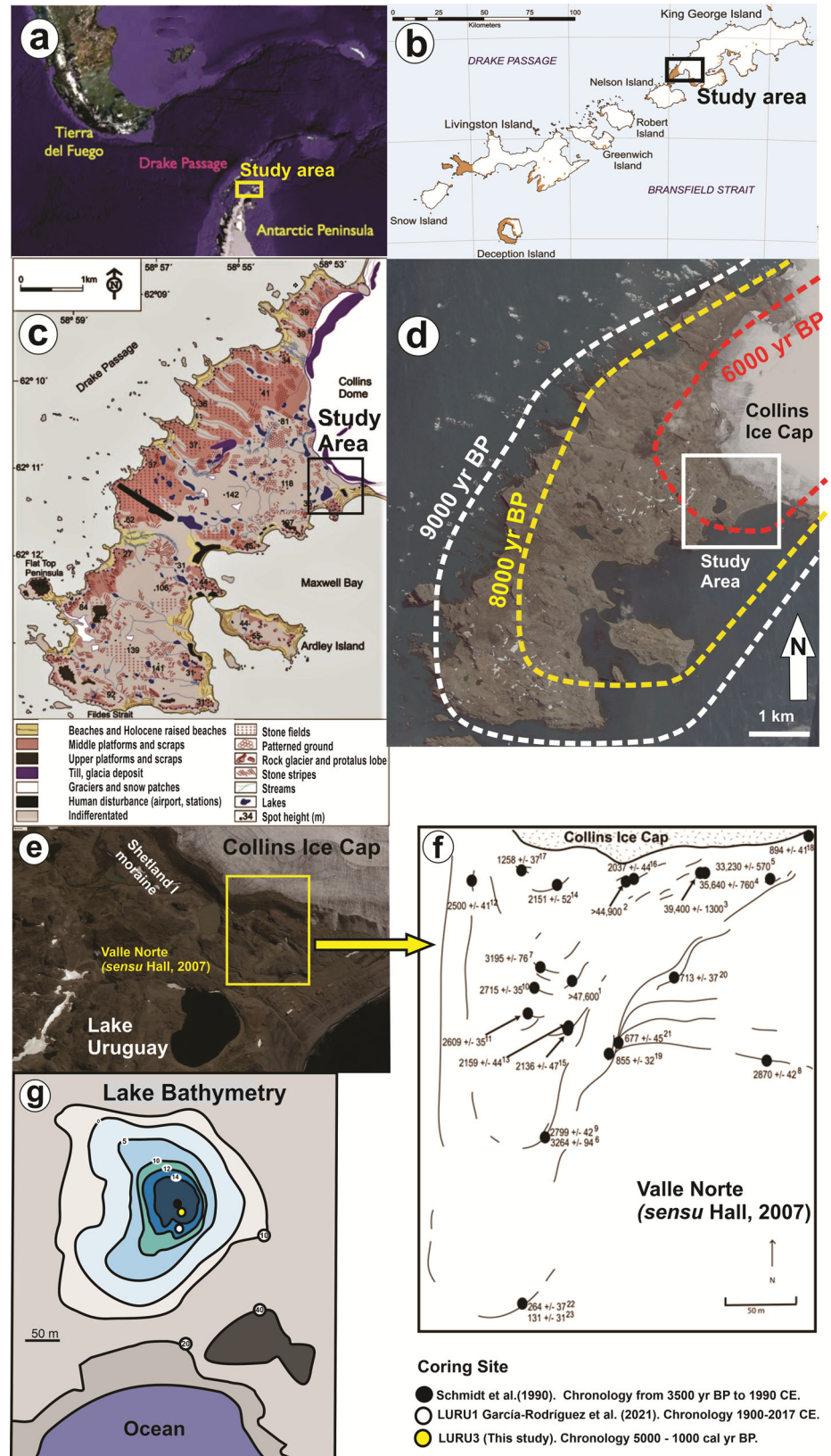
Zone B2 (49 to 30 cm) was characterized by a different community and indicator species represented by *Saccharicenans*, *Methanoregula*, *Carboxydocella* and two ASVs belonging to the Anaerolineaceae family and the Aminicenantes phylum (Table 2, Fig. 4a). This zone showed an increase in species richness and diversity and a decrease in dominance (Fig. 4b). According to the cluster analysis, this zone was subdivided into a lower sub-zone B2a (49 to 36 cm) and an upper B2b (35 to 30 cm) with differences in ASV richness and diversity that were slightly higher in the former subzone.

The third group of ASVs (zone B3, 35-0 cm), was defined by a further increase in richness of *Methanomassiliococcus* and Aminicenantes (Fig. 4b). The ASV indicators were diverse and corresponded to both Bacteria (*Sulfuricella*, *Gallionella*, *Pseudomonas*, *Bellilinea*, *Marispirochaeta* genera, the Caldritrichaceae family, unclassified acidobacteria) and Archaea domains (Euryarchaeota from the *Methanomassiliococcus* and *Methanotherix* genera). The most abundant sequence (ASV 1) within the whole database was the archaeal genus *Methanomassiliococcus*.

## Discussion and perspective

The analysis of geochemistry, stable isotopes and sedaDNA 16 S metabarcoding allowed us to reconstruct the glacier retreat process leading to lake formation and to define three zones related to the Holocene glacier recession process<sup>12-15</sup>. The sill height of Lake Profound is 17.5 m a.s.l. (Watcham et al. 2011) and therefore, the lake was not influenced by the sea water after the last deglaciation<sup>14,16</sup>. Consequently, the paleoenvironmental conditions inferred herein are exclusively interpreted as a glacier recession process. In fact, the identified zones based on geochemical data were coincident with changes in prokaryotic community composition indicating that they are chronologically paralleled. Thus, the basal zone B1 stratigraphically corresponded to G1 (Figs. 2a and 4a), the middle subzones G2a and G2b matched with zone B2a and B2b, respectively, while zone G1 paralleled zone B1. By combining these two lines of evidence, we defined three zones to interpret the Holocene glacier retreat and lake formation (Fig. 1d), namely the basal zone, from the bottom to 50 cm depth (4910–3853 cal yr BP), the middle zone from 50 to 26 cm (3853–2653 cal yr BP), and the upper zone from 26 cm to surface (2653–1074 cal yr BP).

**Fig. 1 | The study area.** **a** Drake Passage (Google Earth Pro, Image Landsat Copernicus); **b** Sub-Antarctic South Shetland Archipelago showing the island ice-free areas;<sup>68</sup> **c** Geomorphological map (modified from Schmid et al. 2017);<sup>44</sup> **d** Holocene migration of Collins Glacier frontline position at 9000, 8000 and 6000 yr BP<sup>13</sup> (Google Earth Pro, Image Landsat Copernicus, copyright 2023 Maxar Technologies. Image U.S. Geological Survey); **e** Aerial photograph of Lake Profound showing the series of moraines of Valle Norte (Google Earth Pro, Image Landsat Copernicus, copyright 2023 Maxar Technologies); **f** Estimated age of the moraine deposits series of Valle Norte; **g** Lake Profound bathymetry showing coring sites of Schmidt et al. (1990)<sup>17</sup> (this study).



Although in a previous work analyzing a different core (LURU1, Fig. 1g) recovered from the same lake, we were able to perform <sup>210</sup>Pb<sup>20</sup> dating, in the attempts on the sediment core reported here, we detected no <sup>210</sup>Pb activity. As shown in Table 1, a subsurface sample from 3 cm depth was dated at ca. 1000 yr BP (Table 1); thus, a possible explanation for the lack of <sup>210</sup>Pb signal

could be a fieldwork coring artifact, i.e., introducing the piston-corer ca. 50 cm below the sediment surface before locking the piston. This would have caused the loss of the uppermost part of the sediment core, where <sup>210</sup>Pb activities should have been detected. We therefore performed an age-depth model using the radiocarbon data (Supplementary Data 1, Fig. 3, Table 1).

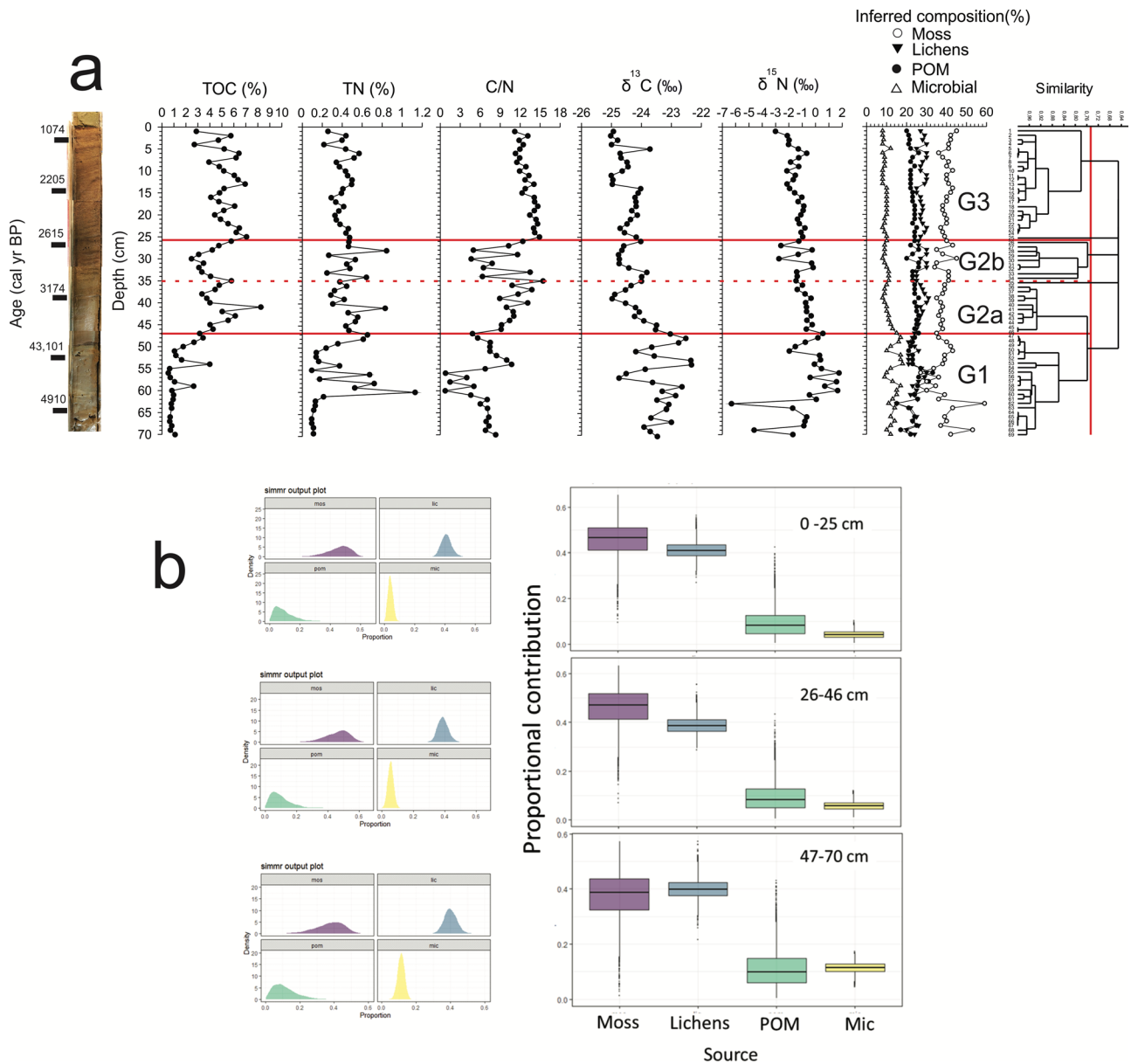


**Fig. 2 | Sedimentary organic matter.** Vertical distribution of TOC, TN, C/N and associated stable isotopes (a). Relative contribution (%) derived from the SIMMR model of potential sources including moss ( $n = 22$ ), lichens ( $n = 26$ ), particulate organic matter (POM), and microbial mats ( $n = 3$ ; MIC) to the sedimentary organic

matter (SOM) in the Antarctic environment (b). Fractionation factors applied<sup>52</sup>,  $\delta^{13}\text{C} = 0.0\text{‰} \pm 0.1$ ;  $\text{C/N} = 0.0$ . The boxes indicate 95%, 75%, 25%, and 5% confidence intervals, respectively.

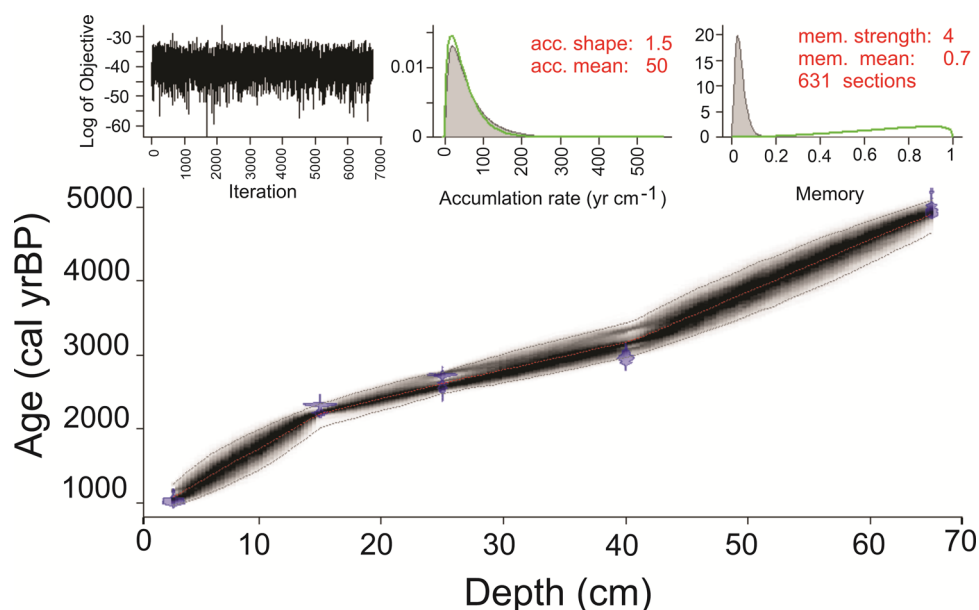
Different aspects of Holocene proglacial lake formation around the frontline of Collins Glacier were already addressed by refs. 12–14 and 15. The reconstruction of the glacier frontline migration in these studies (Fig. 1d) indicates that Lake Profound’s formation can be assigned to the middle Holocene. Based on the increase in TOC concentration and abundance/composition of diatom valves, Schmidt et al. (1990) inferred the onset of genuine limnological conditions after 3155 yr BP and attributed this process to increased glacier erosion and sediment influx due to warming temperatures<sup>17</sup>. Studies in Fildes Peninsula using diatoms preserved in sediments<sup>11,17–19</sup> have illustrated the extent of these environmental changes. However, in the context of paleolimnological studies, prokaryotic communities have received far less attention<sup>20</sup> and our study represents the first with such a detailed and interlinked chronology between geochemical and microbial proxies.

Previous studies proposed that 6000 yr BP, the frontline position of the Collins Glacier was located 1 km further south west than the present, and

that the current frontline was first attained at approximately 5000 yr BP<sup>13</sup> (Fig. 1d, e). Although based on different kind of data (spatial vs. a single habitat chronosequence), the lowest ASV richness and diversity found in this glacier-covered phase (4910–3853 cal yr BP) seems to be in line with the findings of Cauvy-Fraunié and Dangles (2019), who studied global biodiversity and demonstrated that taxon abundance and richness generally increase at lower levels of glacier influence. The authors propose that glacier retreat would increase local biodiversity in the newly formed lakes and that the observed increased richness is mostly explained by the rise in generalist taxa, whereas specialist, ice-dwellers organisms are lost<sup>3</sup>. This process was also inferred from our microbial dataset, where the lower richness of this glacier-covered phase appears to be related to the decrease in specialist bacteria. Moreover, Bosson et al.<sup>21</sup> have recently proposed that ecosystems that emerge after deglaciation will be characterized by extreme to mild ecological conditions, offering refuge for cold-adapted species or favoring generalist species. In fact, the most abundant taxon in the B3 zone is the

**Table 1 | Radiocarbon dates on organic matter from sediment core LURU3, and calculated sedimentation rate from the Bacon age-depth modelling**

Sample number	Depth (cm)	Raw $^{14}\text{C}$ age (yr BP)	2 $\sigma$ 95% (cal yr BP)	Weighted average age (cal yr BP)	Sedimentation rate (mm yr $^{-1}$ )
D-AMS 046936	3	1171 $\pm$ 26	963.3–1255.9	1074	0.03
D-AMS 047727	15	2324 $\pm$ 24	2022–2341.8	2205	0.11
D-AMS 047728	25	2612 $\pm$ 26	2478.6–2768.2	2615	0.24
D-AMS 047729	40	2894 $\pm$ 23	2971–3430.7	3174	0.27
D-AMS 040342	55	39,905 $\pm$ 404	34,662.7–47,510.2	43,101	Excluded
D-AMS 040341	65	4431 $\pm$ 33	4654.7–5086.9	4910	0.14

**Fig. 3 | Bayesian age-depth model for sediment core LURU3.** The central panel shows the calibrated  $^{14}\text{C}$  dates (transparent blue), and the age-depth model grey stippled lines indicate the 95% confidence intervals; the red curve shows the best possible fit based on the weighted mean age for each depth.

archaea *Methanomassilicoccus*, which based on comparative genomics has been described as generalist<sup>22</sup>.

The presence of gravel clasts and fine sand indicates the existence of a terrestrial environment under the active influence of the glacier front. This inference is supported by the occurrence of ASV with closest relative species in the database to bacterial taxa typical for soils or Antarctic rocks. Among them, some species of the genus *Methylobacterium* hold the capacity of fixing atmospheric nitrogen and others are endophytes. In Antarctica, *Methylobacterium* strains occur more often associated with mosses, lichens and in the rhizosphere of *Deschampsia antarctica* than in lakes<sup>23</sup>. This agrees with the fact *Methylobacterium* has a high resistance to UV radiation and dehydration<sup>24</sup>, which are two common environmental stressors of Antarctica.

*Sphingomonas* strains have been isolated from soil samples in Fildes Peninsula (Geng et al., 2019), Antarctic hypoliths<sup>25</sup> and, more recently, sequences belonging to Sphingomonadaceae were found to be very abundant in the rhizosphere of Antarctic plants<sup>26</sup>. The characteristics of the microbial groups recorded here through the sedaDNA metabarcoding approach agree with their terrestrial origin.

The type of sedimentary facies of this zone was described by Hall (2007) as ridges rich in clay- or sand-rich till with gravel and cobble clasts and interpreted as moraine deposits of either thrust blocks of marine and outwash fan sediments<sup>12</sup>.

The unexpected Pleistocene age at 55 cm depth and the high relative abundance of a single ASV affiliated to *Herbaspirillum huttense*, suggest the presence of pristine soils because this genus has been regarded to as an indicator of these conditions in Antarctica<sup>27</sup>. This older sediment structure was already identified by Hall (2007) in the catchment of Lake Profound<sup>12</sup>

(Fig. 1e, f) where at least four moraine deposits yielded an age older than 33,000 yr BP. Such moraines were described as non-in situ thrust-up (or outwash fan sediment) from marine origin (Table 1, Supplementary Table 1).

The middle section of this zone showed the highest POM values together with the lowest C/N ratios, probably indicating eventual inputs of glacial flour and the occurrence of a moraine deposit actively connected to the glacier front. The lowest diversity and species richness indicate that glacier-frontline biotopes would exhibit rather unfavorable ecological conditions for bacterial development than those of proglacial lakes. Above 55 cm depth, the increase in TOC and prokaryotic diversity and richness flags the transition to the next zone (3853 to 2653 cal yr BP).

In this middle zone, the increase in both TOC and TN indicates a more intense biological colonization than that of the previous zone, as also suggested not only by the visualized moss content within the sediment core, but also by the increase in C/N ratios, as observed by other studies in nearby areas<sup>20,28</sup>. Such a shift in sedimentary organic matter composition indicates the beginning of the separation process of the moraine from the glacier front, and the onset of more genuine limnological conditions, expressed perhaps as a small proglacial shallow lake. These conditions, more favorable for the establishment of microbial communities than those from the glacier forefield, were confirmed by the increase in prokaryotic diversity and richness compared with the glacier-dominated zone (i.e., B1).

After a glacier retreat and loss of hydrological connectivity, the newly created lake usually undergoes changes from a turbid (due to suspended mineral particles from the glacier runoff) to a clear lake phase<sup>29</sup>. During the turbid phase, primary production is expected to be low because of light limitation and the biota of these lakes consists mainly of heterotrophic

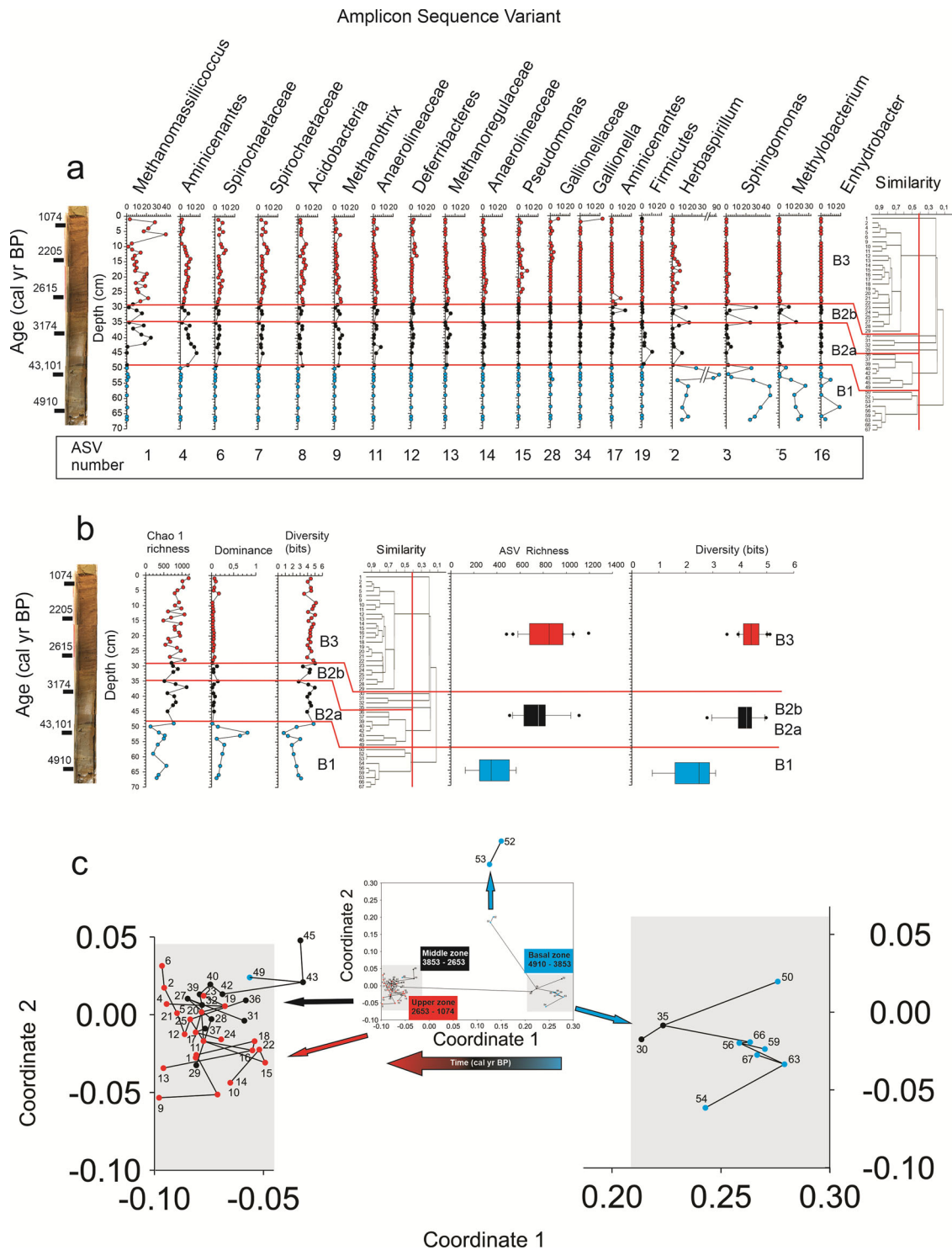


**Fig. 4 | Prokaryotic community.** ASVs accounting for 50% of the relative abundance in the different zones identified by cluster analysis (a). ASV richness, Dominance and Shannon diversity ( $H'$ ) found through the core and for each identified zone (box plots showing the median; upper and lower quartiles and outliers) (b). Non-metric multidimensional scaling (NMDS) ordination of the prokaryotic

community composition (ASVs) based on Bray-Curtis distances (stress = 0.10,  $r^2$  of 0.81 and 0.12 for the coordinate 1 and 2, respectively) between samples. Samples are coded according to the sediment depth (in cm) in the core and the zones B1, B2 and B3. The minimum spanning tree is shown (black line) (c).

microbes<sup>30</sup>. Once the suspended material eventually settles down, the water column becomes clear and these changes in the physical and chemical environment induce a shift in microbial community composition<sup>30,31</sup>. This transition process from glacier-dominated to a turbid and later onset of a clear lake, together with the concomitant changes in microbial community composition, is reflected in the changes of indicator species. Thus, we

detected several ASVs with a high identity similarity with sequences obtained from Andean lakes (Table 2) affiliated to genera from Aminicenantes (KY690858), Firmicutes (KY692172), Chloroflexi (KY692022), and Euryarchaeota phyla (KY690699). Aminicenantes and Chloroflexi bacterial genomes have been assembled from Siberian permafrost metagenomes and show adaptations to the long-term energy starvation normally observed in

**Table 2 | High abundance ASVs (see Fig. 4) showing significant differences between the three detected sample groups (see cluster and box plots in Fig. 4a, b) and assigned as indicator species for each group (IndVal: Specificity >50%, Fidelity >90%,  $p < 0.01$ )**

ASV	Zone	GenBank Closest Relative (% Identity), Accession Number	Origin	Identification according to RDP Classifier [% Bootstrap support]
1	B3	Archaea (100%), KC875576	Sediment	<i>Methanomassiliococcus</i> [96%]
6	B3	Unc. bacterium clone (99%), LK025462	Sediment, Peat soil	<i>Marispirochaeta</i> [60%]
7	B3	Unc. bacterium clone (99%), LK025462	Sediment, Peat soil	<i>Marispirochaeta</i> [65%]
8	B3	Unc. bacterium clone (98%), JQ793192	Sediment	<i>Acidobacteria_Gp16</i> [40%] Gp16[40%]
9	B3	Unc. Methanosaeta sp (100%), KX463152	Sediment	<i>Methanotrix</i> [100%]
12	B3	Unc. bacterium clone (96%), AB656785	Rice paddy soil	Calditrichaceae [26%]
14	B3	Unc. bacterium clone (99%), DQ463268	Sediment	Anaerolineaceae [98%] <i>Bellilinea</i> [32%]
15	B3	<i>Pseudomonas</i> sp. (100%), OP890955	Soil	<i>Pseudomonas</i> [100%]
34	B3	Unc. beta proteobacterium (99%), HE858171	Groundwater	<i>Gallionella</i> [100%]
28	B3	Unc. bacterium clone (99%), KY690625	Sediment	<i>Sulfuricella</i> [97%]
4	B2	Unc. bacterium clone (99%), KY690858	Sediment	<i>Saccharicenans</i> [72%]
13	B2	Unc. bacterium clone (99%), KY690699	Sediment	<i>Methanoregula</i> [85%]
11	B2	Unc. bacterium clone (100%), KY692022	Sediment	Anaerolineaceae [99%]
17	B2	Unc. bacterium clone (100%), KY690718	Sediment	Aminicenantes_genera_incertaines_sedis [47%]
19	B2	Unc. bacterium clone (99%), KY692172	Sediment	<i>Carboxydocella</i> [24%]
2	B1	<i>Herbaspirillum huttiense</i> (100%), MN420775	Soil, Water	<i>Herbaspirillum</i> [100%]
3	B1	<i>Sphingomonas</i> sp. (100%), MN865727	Antarctic rocks	<i>Sphingomonas</i> [100%]
5	B1	<i>Methylobacterium</i> sp. (100%), LC546612	Soil	<i>Methylobacterium</i> [100%]
16	B1	<i>Moraxella</i> sp. (100%) MN833048	Sediment	<i>Enhydrobacter</i> [100%]

Unc., uncultured.

frozen environments<sup>32</sup>. Aminicenantes bacteria can be found in environments with a wide range of oxygen concentration, whereas Clostridia are strictly anaerobic. Members of the Firmicutes phylum are very abundant in meltwater from a glacial lake outburst flood<sup>33</sup>. Among these bacteria, the ASV 19 belongs to Clostridia and was putatively and preliminary affiliated to the *Carboxydocella* genus (low bootstrap support), an obligate anaerobe bacterial genus able to reduce Fe<sup>3+</sup> associated to biogeochemical cycles in volcanic remains from Antarctic glaciers<sup>34</sup>. In the case of the Euryarchaeota indicator, which according to RDP classifier would be affiliated to the *Methanoregula* genus (85% bootstrap support), a methanogenic hydrogenotrophic archaeon recorded in sub-Antarctic freshwater ecosystems<sup>35</sup>. The presence of both aerobic and anaerobic prokaryotic indicator groups from ice, melt-water and lake water strongly suggests that sedaDNA samples represent a transitional fluctuating stage from a glacier front to a moraine and proglacial lake deposit. For example, subglacial sediments are assumed to be largely anoxic<sup>36</sup>, while the recently formed turbid lakes are oxygenated. This would explain the concomitant presence of bacteria and archaea with contrasting metabolisms.

The variability in C/N ratios between terrestrial and aquatic organic matter<sup>37</sup> in this section further supports the inference of intermittent proglacial-lake conditions. This is also in agreement with previous studies, which concluded that the glacier front was located 400 to 500 m beyond the present-day glacier position, and therefore, at that time the connection of Lake Profound to the glacier was still active<sup>12</sup>. Therefore, this zone is interpreted as a scenario of glacier recession and onset of early stages of a proglacial lake, but still at least intermittently connected to the glacier until ca. 2600 cal yr BP, where the transition to the uppermost zone was inferred.

A recent study addressing microbial community composition in Fildes Peninsula lakes<sup>38</sup> observed that bacterioplankton richness was higher under ice-covered conditions than during warmer seasons. This suggests that rainfall and glacier runoff inputs to the lakes during summer, transport organic matter that is not readily available for lake bacteria<sup>38</sup>. This generates measurable changes in the plankton community structure, which are then

reversed when the lake is further covered by ice and the available organic matter is mainly autochthonous. Similarly, glacier advance and retreat appear to provoke changes in the sources of organic matter, thus influencing the composition of the bacterioplankton.

Finally, the C/N ratio stabilization together in the upper zone (2653 – 1074 cal yr BP) with the visual moss content and the distinct series of silt-lamination clearly shows the initial stages of stable lake conditions and the loss of an active connection with the glacier frontline. The highest and most stable TOC and TN values observed here indicate a most intense biological colonization within the lake until ca. 1000 cal yr BP. Accordingly, this zone showed the highest values of prokaryotic richness and diversity. Shannon diversity values were similar to those already described for the bacterioplankton community from lakes of Fildes Peninsula<sup>38</sup>. In addition, the indicator ASVs showed more diverse metabolic abilities than those of the previous zones and included methanogenic archaea (*Methanomassiliococcus*, *Methanotrix*), aquatic (*Marispirochaeta*, *Gallionella*, *Sulfuricella*, Calditrichaceae) and sediment (*Bellilinea*) bacteria, suggesting the occurrence of a highly diverse, well-established lake microbial community. Thus, the onset of genuine limnological conditions was particularly flagged by the stabilization of C/N ratios and maximum bacteria richness and diversity.

Our findings indicate that the transition from a glacier-dominated environment to a lake affected the structure and composition of the prokaryotic community, and that species turnover (species replacement) hierarchically contributed more than nestedness did (species loss) to the observed differences among different times (Fig. 5). Similar findings were reported for the bacterial communities along a chrono-sequence in an Arctic glacier forefield, where a strong turnover of bacterial communities was recorded and the changes were particularly rapid during the first years after the retreat of the glacier<sup>39</sup>. Whether the observed species replacement through time is due to either taxonomic turnover within the same functional group, or to the environmental heterogeneity (drastic environmental change between the different stages) is still an open question, as thorough measurements of other environmental variables should be accordingly done<sup>40</sup>.

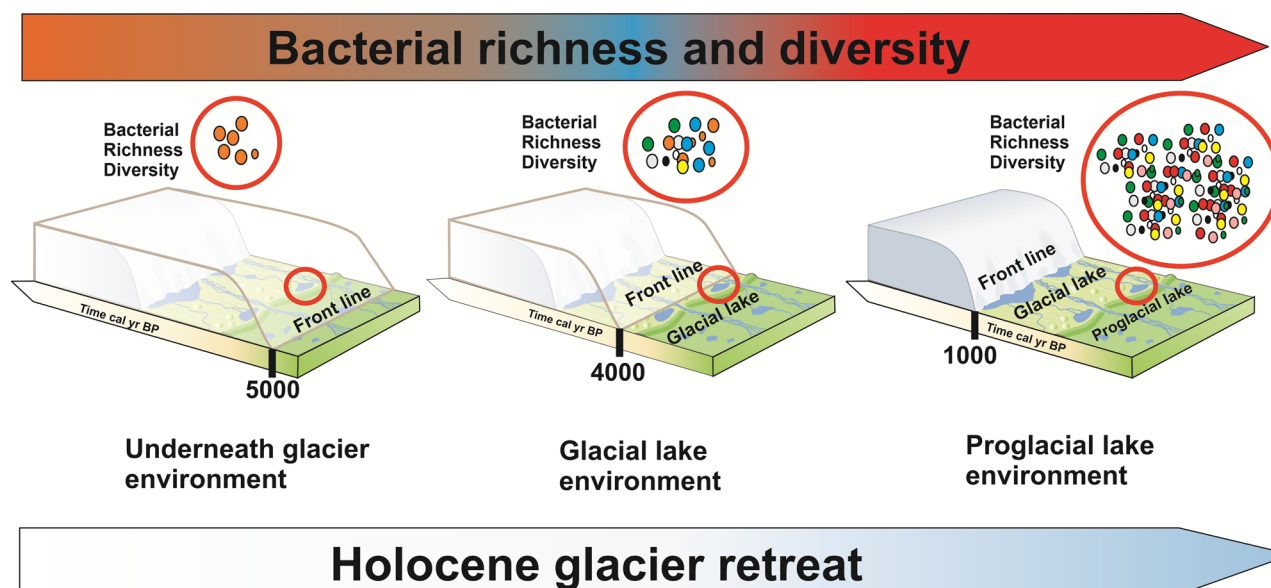


**Fig. 5 | Scheme of the Holocene Antarctic glacier retreat process and associated changes in bacterial richness and diversity.** Left: glacier environment exhibiting the lowest bacterial diversity and richness at ~5000 cal yr BP. Center: transition to a glacial lake environment that was associated with an increase in bacterial richness

and diversity. Right: the highest bacterial diversity and richness found after the onset of a proglacial lake fully separated from the Collins Glacier. The chronology of glacier retreat is in accordance with Fig. 1 as inferred from Ref. 13.

Major limitations of using sedaDNA and metagenomic approaches are the uncertainty about the DNA origin, physiological state of the original cell (dormant or dead cells)<sup>41</sup> and the preservation state. Depending on the state of degradation, which is affected by temperature, age, oxygen availability, pH, and mineral composition of sediments<sup>42</sup>, the DNA can be retrieved in a well-preserved state (recent sediments) or as sedaDNA, which is usually more poorly preserved. Nonetheless, several studies have shown that the application of 16 S metabarcoding to sedaDNA is a reliable methodology for inferring the microbial diversity in samples of lacustrine sediments<sup>43</sup>, but also for reconstructing the past microbiota of the lakes. Here, we were able to extract DNA from 4910 to 1074 cal yr BP suitable for 16S rRNA metabarcoding. While the age of the samples could have biased the recovery of DNA suitable for paleoanalysis, the richness and diversity values calculated for the oldest samples, although lower than in the subsequent zones, suggest an efficient DNA recovery (Fig. 4b).

In conclusion, the retrieved information on geochemistry, stable isotopes and sedaDNA metabarcoding allowed us to reconstruct with detail the different Holocene stages of Collins Glacier forefield and infer the formation of Lake Profound. The prokaryotic and geochemical signals characteristic of each stage can be effectively used in further studies as baseline proxies of pristine conditions.

## Methods

### Study site

The South Shetland archipelago is located in the subantarctic belt on the Drake Passage (Fig. 1a) and consists of six major islands, which exhibit a number of warm-season transitional ice-free areas mostly set on the east side of each island (Fig. 1b). Such transitional areas are actually very unusual in the whole Antarctic continent and are characterized by the occurrence of moraine deposits and proglacial lakes (Fig. 1c). In the case of Fildes Peninsula, proglacial lakes are normally small and some of them still display an active connection to the Collins Glacier (Fig. 1c and e), but others, such as Lake Profound, lost the active connection and are instead fully separated from the ice cap. It lies 18 m a.s.l., it is ca. 0.05 km<sup>2</sup>, and has a maximum depth of 14.7 m<sup>14,17,18</sup>, Fig. 1g). The geomorphology indicates that the occurrence of permafrost is closely linked to periglacial processes (Fig. 1c). The active periglacial landforms account for one third of the peninsula and

are mainly located on more elevated platforms of marine origin (i.e., 30–50 m a.s.l.), where cryoturbation is considered as the main process<sup>20,44</sup>.

The Holocene process of deglaciation within the Fildes Peninsula (Fig. 1d) has been inferred by Mäusbacher et al. (1989) and confirmed by Oliva et al. (2023). They proposed three main stages of the Collins Ice Cap frontline position. By 9000 yr BP, the frontline position was located on the surrounding southwestern most tip of the peninsula<sup>13,15</sup>. Towards 8000 yr BP, the frontline had migrated about 1 km towards the center of the peninsula and by 6000 yr BP, the frontline position had shifted to about 500 m away from the position of Lake Profound. This process of frontline migration was explained due to a combination of both climate warming and sea level rise control<sup>14,45</sup>. In this regard, Hall (2007) also inferred that by 3500 yr BP the frontline position had migrated to 400 to 500 m southwest away from the contemporary frontline position. This means that Lake Profound's formation can be assigned to the middle Holocene<sup>12</sup>.

The land located between the lake and the Collins Glacier known as the Valle Norte area (Fig. 1e, f) exhibits a series of small moraines and drift deposits located ~300–500 m away from the present-day margin and are expressed as small depressions obliquely set to the glacier orientation. Between this landform and the glacier, there are discontinuous moraine blocks of 1–5 m of relief which are usually sharp-crested and asymmetric (Fig. 1e, f). Although the outer ridges consist of clay/sand-rich till with gravel and cobble clasts, most inner moraines are thrust blocks of marine and outwash fan sediments. Marine sediments contain massive clay, as well as interbedded silt and sand. The age of all of these moraine deposits ranges between 3200 to 890 yr BP, although there are several older spots exhibiting ages ranging between 47,200 to 33,200 yr BP and interpreted as marine deposits (Fig. 1f)<sup>12</sup>.

### Sampling

A 70-cm-long sediment core was obtained in March 2019 using a 63 mm internal diameter UWITEC piston corer located on a floating platform above the deepest point of the lake. The tube was sealed hermetically for transport to the laboratory. Once in the laboratory, the core tube was thoroughly cleaned with 70% ethanol and opened lengthwise in a clean room using cutters that were previously ethanol-treated. The core was cut every 1 cm sections and immediately placed in sterile whirl pack bags. To



preclude contamination during sampling, the most outer sediment in contact with the core was excluded. A single core is considered suitable to study the temporal dynamics of prokaryotes, since they are evenly distributed in the water column<sup>43</sup>.

### Geochronology

A total of six sediment samples for AMS <sup>14</sup>C dating on bulk organic matter were first dispersed and sieved to attain homogeneity and then treated with HCl to remove carbonates, rinsed to neutrality and finally lyophilized for combustion. Dry aliquots were subject to combustion to CO<sub>2</sub> according to the previously estimated carbon content, to generate gas equivalent to 1–2 mg carbon. The resulting CO<sub>2</sub> was transferred to a sealed tube containing iron and zinc to form graphite following the Bosch reaction. Graphite was compressed into instrument-specific targets and measured by a 500 kV National Electrostatics Corporation 1.5 SDH Compact Pelletron AMS. Laboratory number of all samples is provided in Supplementary Data 1. The age-depth modelling was done using the radiocarbon data with the free Bacon software using the SHCal13 Southern Hemisphere calibration curve<sup>46,47</sup>. Briefly, the core was divided in many thin vertical sections (by default of res=5 cm thickness), and then, the accumulation rate (in years/cm) for each of these sections was estimated using Markov Chain Monte Carlo (MCMC) iterations. The Bacon software provides functions to obtain accumulation rates (in years per cm, meaning sedimentation times)<sup>46,48</sup>.

### Stable isotopes

Carbon (<sup>13</sup>C/<sup>12</sup>C, referred as δ<sup>13</sup>C) and nitrogen (<sup>15</sup>N/<sup>14</sup>N, or δ<sup>15</sup>N) stable isotope ratios were analyzed simultaneously<sup>48</sup> at the Integrated Analysis Centre (CIA-FURG). Samples were freeze-dried, ground and homogenized, and approximately 1 mg of sediment was placed into tin capsules. An isotope-ratio mass spectrometer EA Flash 2000 Delta V Advantage-ThermoFisher Scientific coupled to an elemental analyzer was used for the stable isotope analysis of carbon and nitrogen. Values are provided in delta notation (δ), expressed in ‰ following Bond and Hobson (2012)<sup>49</sup>, with VPDB (Vienna Pee Dee Belemnite limestone) as the international standard for carbon and AIR for nitrogen, in addition to glutamic acid, caffeine, acetanilide and the internal laboratory standards. To identify the contribution of each organic matter source within the lagoon sediments, Bayesian SI mixing model in the SIMMR package<sup>50</sup> was used. This application has been successfully used for estimation of sources contribution in sediments<sup>51–53</sup>. The SIMMR model was run using δ<sup>13</sup>C and C/N values through 10,000 iterations with the Markov Chain Monte Carlo (MCMC) algorithm. Based on δ<sup>13</sup>C and C/N values, this analysis determines the probability of source proportions contribution in the recorded sample while accounting for uncertainty (e.g., isotopic fractionation, diagenetic alterations, residual error). SIMMR analysis included the absolute ratio of C/N and δ<sup>13</sup>C values in sediments since these components are not susceptible to large diagenetic fractionation, while δ<sup>15</sup>N values are more affected by diagenetic process in sediments<sup>52,54,37</sup>. In this context, we assumed a conservative standard error (0.0‰ ± 0.1‰<sup>52</sup>.

We considered basal sources that are present in our sampling sites in Antarctic environments including the mean isotopic values of 22 species of mosses and 26 species of lichens reported by Lee et al. (2009)<sup>55</sup>, microbial mats collected in the Fildes Peninsula from<sup>56</sup>, and particulate organic matter (POM) from surface coastal waters of Collins Bay<sup>57</sup>.

### Sedimentary ancient DNA (sedaDNA) extraction and 16S rRNA gene sequencing

A total of 46 sediment subsamples (300 mg) were transferred with autoclaved stainless-steel spoons into sterile plastic tubes containing 800 μL of lysis buffer: 100 mM Tris-HCl, 100 mM EDTA, 100 mM Na-Phosphate (pH 8.0), 1.5 M NaCl and 1% CTAB. The mix was agitated for 40 s at 6 m s<sup>-1</sup> in a FastPrep homogenizer (MP Biomedicals), centrifuged to discard the debris, and the supernatant was applied to a PurePrep 32 (Molgen)<sup>58</sup> for sedaDNA purification. All sedaDNA extraction steps were done under vertical laminar flow cabinets (ESCO Class II, Type A2) located in a separate room

exclusively used for DNA- and RNA-based studies and whose surfaces were previously irradiated for 30 min using the built-in UV lamp.

The sedaDNA concentration and quality were checked using a NanoDrop spectrophotometer. As bacteria are likely the first organisms colonizing newly formed proglacial lakes<sup>29</sup>, we have applied 16S metabarcoding to the sedaDNA in order to determine the prokaryotic community composition through the sediment core (and therefore through time). Amplicon sequencing of the V4 hypervariable region of the 16S RNA gene was done with primers 515 forward and 806 reverse at Novogene using the NovaSeq PE250 Illumina platform (Illumina, San Diego, CA, USA).

### Sequences and data analysis

The obtained reads were analyzed in R using the DADA2 pipeline<sup>59,60</sup>. Adapter sequences, barcodes, primers, and the first 15 bp were removed from the reads. Then, the reads were filtered based on the sequence quality (quality score > 25) and amplicon size. Sequence variations were inferred and assigned to Amplicon Sequence Variants (ASV) at the level of single-nucleotide differences. Chimeric sequences were eliminated, and taxonomy assignments were performed based on the SILVA database (v138)<sup>61</sup>. Those ASV whose abundance was less than or equal to five in the total number of samples were eliminated.

Alpha diversity indices (richness, Shannon H' and Chao1) were calculated using the relative abundance of ASVs in each sample. Differences between the alpha diversity indexes calculated for each zone (B1, B2, B3) were analyzed using mixed effect models (differences were considered significant for *p* values < 0.05<sup>62</sup>).

Beta diversity was analyzed according to non-metric multidimensional scaling (NMDS) based on Bray-Curtis distances. The turnover of species among depth samples was estimated using presence/absence data (P/A). Diversity analyses were done using the R package Vegan<sup>63</sup>. Sorensen beta diversity index (β<sub>SOR</sub>) was calculated as the overall turnover of species, which was decomposed into two different components: nestedness (β<sub>NEST</sub>) and Simpson's similarity (β<sub>SIM</sub>). Nestedness (β<sub>NEST</sub>) represent the loss of species between sites, and can be used to test the exclusion of species caused by strong environmental filters. Similarity (β<sub>SIM</sub>) represent the fraction of turnover caused by changes in the identity of the species between sites<sup>64,65</sup>.

A stratigraphically constrained cluster analysis (which allows only adjacent depths to be joined during the agglomerative clustering procedure) was done with Past 4.03<sup>66</sup> using the UPGMA algorithm and the Morisita similarity index. Zones were set at 75% similarity for geochemical data and at 40% for ASV data. According to the grouping inferred for the geochemical variables (vertical distribution of TOC, TN, C/N and associated element stable isotopes), a Permanova test based on the Bray-Curtis similarity index (9999 permutations) was ran to determine the strength of the grouping.

Based on the ASVs accounting for 50% of total sample abundance, the indicator species analysis (IndVal) was applied for identifying the ASVs indicative of each zone (implemented on Past v. 4<sup>66,67</sup>). The selected indicator ASVs were those showing significant values (*p* < 0.05), specificity > 50% and fidelity > 90%.

### Reporting summary

Further information on research design is available in the Nature Portfolio Reporting Summary linked to this article.

### Data availability

Total organic carbon (TOC), total nitrogen (TN), <sup>13</sup>C and <sup>15</sup>N isotopes from sediment samples, as well as the obtained DNA concentrations and the radiocarbon data used to generate the age model are stored in <https://doi.org/10.6084/m9.figshare.24968994.v2>. The 16S rRNA obtained sequences are in the PRJNA945065 project of GenBank database (<https://www.ncbi.nlm.nih.gov/bioproject/PRJNA945065/>).

Received: 27 July 2023; Accepted: 29 January 2024;

Published online: 21 February 2024

## References

- Stibal, M. et al. Glacial ecosystems are essential to understanding biodiversity responses to glacier retreat. *Nat. Ecol. Evol.* **4**, 686–687 (2020).
- Milner, A. M. et al. Glacier shrinkage driving global changes in downstream systems. *Proc. Natl. Acad. Sci.* **114**, 9770–9778 (2017).
- Cauvy-Fraunié, S. & Dangles, O. A global synthesis of biodiversity responses to glacier retreat. *Nat. Ecol. Evol.* **3**, 1675–1685 (2019).
- Azam, F. et al. The ecological role of water-column microbes in the sea. *Mar. Ecol. Prog. Ser.* **10**, 257–263 (1983).
- Fenchel, T. The microbial loop—25 years later. *J. Exp. Mar. Bio. Ecol.* **366**, 99–103 (2008).
- Glibert, P. M. & Mitra, A. From webs, loops, shunts, and pumps to microbial multitasking: Evolving concepts of marine microbial ecology, the mixoplankton paradigm, and implications for a future ocean. *Limnol. Oceanogr.* **67**, 585–597 (2022).
- Grossart, H.-P., Massana, R., McMahon, K. D. & Walsh, D. A. Linking metagenomics to aquatic microbial ecology and biogeochemical cycles. *Limnol. Oceanogr.* **65**, S2–S20 (2020).
- Margesin, R. & Collins, T. Microbial ecology of the cryosphere (glacial and permafrost habitats): current knowledge. *Appl. Microbiol. Biotechnol.* **103**, 2537–2549 (2019).
- Crump, S. E. Sedimentary ancient DNA as a tool in paleoecology. *Nat. Rev. Earth Environ.* **2**, 229 (2021).
- Holland, P. R., Bracegirdle, T. J., Dutrieux, P., Jenkins, A. & Steig, E. J. West Antarctic ice loss influenced by internal climate variability and anthropogenic forcing. *Nat. Geosci.* **12**, 718–724 (2019).
- Watcham, E. Late Quaternary relative sea level change in the South Shetland Islands, Antarctica. Doctoral thesis. (Durham University, 2010).
- Hall, B. L. Late-Holocene advance of the Collins ice cap, King George Island, South Shetland islands. *The Holocene* **17**, 1253–1258 (2007).
- Mäusbacher, R., Müller, J. & Schmidt, R. Evolution of postglacial sedimentation in Antarctic lakes (King George Island). *Zeitschrift für Geomorphol.* **33**, 219–234 (1989).
- Watcham, E. P. et al. A new Holocene relative sea level curve for the South Shetland Islands, Antarctica. *Quat. Sci. Rev.* **30**, 3152–3170 (2011).
- Oliva, M. et al. Holocene deglaciation of the northern Fildes Peninsula, King George Island, Antarctica. *L. Degrad. Dev.* **34**, 3973–3990 (2023).
- Watcham, E. Late Quaternary Relative Sea Level Change in the South Shetland Islands, Antarctica. (Durham University, 2010).
- Schmidt, R., Mäusbacher, R. & Müller, J. Holocene diatom flora and stratigraphy from sediment cores of two Antarctic lakes (King George Island). *J. Paleolimnol.* **3**, 55–74 (1990).
- Oaquim, A. B. J., Moser, G. A. O., Evangelista, H., Licínio, M. V. & Van De Vijver, B. *Aulacoseira glubokoyensis* sp. nov. (Bacillariophyceae), a new centric diatom from the Maritime Antarctic region. *Phytotaxa* **328**, 149–158 (2017).
- Van de Vijver, B. & Beyens, L. Biogeography and ecology of freshwater diatoms in Subantarctica: a review. *J. Biogeogr.* **26**, 993–1000 (1999).
- García-Rodríguez, F. et al. Centennial glacier retreat increases sedimentation and eutrophication in Subantarctic periglacial lakes: A study case of Lake Uruguay. *Sci. Total Environ.* **754**, 142066 (2021).
- Bosson, J. B. et al. Future emergence of new ecosystems caused by glacial retreat. *Nature* **620**, 562–569 (2023).
- de la Cuesta-Zuluaga, J., Spector Tim, D., Youngblut, N. & Ley, R. Genomic Insights into Adaptations of Trimethylamine-Utilizing Methanogens to Diverse Habitats, Including the Human Gut. *mSystems* **6**, <https://doi.org/10.1128/msystems.00939-20> (2021).
- Romanovskaia, V. A., Rokitko, P. V., Shilin, S. O., Chernaia, N. A. & Tashirev, A. B. Distribution of bacteria of *Methylobacterium* genus in the terrestrial biotopes of the Antarctic region. *Mikrobiol. Zh.* **71**, 3–9 (1993).
- Tahon, G. & Willems, A. Isolation and characterization of aerobic anoxygenic phototrophs from exposed soils from the Sør Rondane Mountains, East Antarctica. *Syst. Appl. Microbiol.* **40**, 357–369 (2017).
- Gunnigle, E., Ramond, J.-B., Guerrero, L. D., Makhalyane, T. P. & Cowan, D. A. Draft genomic DNA sequence of the multi-resistant *Sphingomonas* sp. strain AntH11 isolated from an Antarctic hypolith. *FEMS Microbiol. Lett.* **362**, 1–4 (2015).
- Prekrasna, I. et al. Antarctic Hairgrass Rhizosphere Microbiomes: Microscale Effects Shape Diversity, Structure, and Function. *Microbes Environ.* **37**, Article ME21069 (2022).
- Wang, N. F. et al. Diversity and structure of soil bacterial communities in the Fildes Region (maritime Antarctica) as revealed by 454 pyrosequencing. *Front. Microbiol.* **6**, 1–11 (2015).
- Carrizo, D., Sánchez-García, L., Menes, R. J. & García-Rodríguez, F. Discriminating sources and preservation of organic matter in surface sediments from five Antarctic lakes in the Fildes Peninsula (King George Island) by lipid biomarkers and compound-specific isotopic analysis. *Sci. Total Environ.* **672**, 657–668 (2019).
- Sommaruga, R. When glaciers and ice sheets melt: consequences for planktonic organisms. *J. Plankton Res.* **37**, 509–518 (2015).
- Peter, H. & Sommaruga, R. Shifts in diversity and function of lake bacterial communities upon glacier retreat. *ISME J.* **10**, 1545–1554 (2016).
- Peter, H., Jeppesen, E., De Meester, L. & Sommaruga, R. Changes in bacterioplankton community structure during early lake ontogeny resulting from the retreat of the Greenland Ice Sheet. *ISME J.* **12**, 544–555 (2018).
- Katie, S. et al. Eight Metagenome-Assembled Genomes Provide Evidence for Microbial Adaptation in 20,000- to 1,000,000-Year-Old Siberian Permafrost. *Appl. Environ. Microbiol.* **87**, e00972–21 (2021).
- Ilahi, N. et al. Diversity, distribution, and function of bacteria in the supraglacial region hit by glacial lake outburst flood in northern Pakistan. *Environ. Sci. Eur.* **34**, 73 (2022).
- García-Lopez, E. et al. Microbial Community Structure Driven by a Volcanic Gradient in Glaciers of the Antarctic Archipelago South Shetland. *Microorganisms* **9**, 392 <https://doi.org/10.3390/microorganisms9020392> (2021).
- Lavergne, C. et al. Temperature differently affected methanogenic pathways and microbial communities in sub-Antarctic freshwater ecosystems. *Environ. Int.* **154**, 106575 (2021).
- Stibal, M., Hasan, F., Wadham, J. L., Sharp, M. J. & Anesio, A. M. Prokaryotic diversity in sediments beneath two polar glaciers with contrasting organic carbon substrates. *Extremophiles* **16**, 255–265 (2012).
- Leng, M. J. et al. *Isotopes in lake sediments*. (Springer, 2006).
- Bertoglio, F., Piccini, C., Urrutia, R. & Antoniadou, D. Seasonal shifts in microbial diversity in the lakes of Fildes Peninsula, King George Island, Maritime Antarctica. *Antarct. Sci.* 1–14 <https://doi.org/10.1017/S0954102023000068> (2023)
- Scutte, U. M. E. et al. Bacterial diversity in a glacier foreland of the high Arctic. *Mol. Ecol.* **19**, 54–66 (2010).
- Louca, S. et al. Function and functional redundancy in microbial systems. *Nat. Ecol. Evol.* **2**, 936–943 (2018).
- Prosser, J. I. Dispersing misconceptions and identifying opportunities for the use of ‘omics’ in soil microbial ecology. *Nat. Rev. Microbiol.* **13**, 439–446 (2015).
- Smith, C. I. et al. Not just old but old and cold? *Nature* **410**, 771–772 (2001).
- Capo, E. et al. Lake sedimentary DNA research on past terrestrial and aquatic biodiversity: Overview and recommendations. *Quaternary* **4**, 6 (2021).
- Schmid, T. et al. Geomorphological mapping of ice-free areas using polarimetric RADARSAT-2 data on Fildes Peninsula and Ardley Island, Antarctica. *Geomorphology* **293**, 448–459 (2017).
- Lüning, S., Galka, M. & Vahrenholt, F. The medieval climate anomaly in Antarctica. *Palaeogeogr. Palaeoclimatol. Palaeoecol.* **532**, 109251 (2019).
- Blaauw, M. & Christen, J. A. Flexible paleoclimate age-depth models using an autoregressive gamma process. *Bayesian Anal.* **6**, 457–474 (2011).

47. Hogg, A., Turney, C., Palmer, J., Cook, E. & Buckley, B. Is there any evidence for regional atmospheric  $^{14}\text{C}$  offsets in the Southern Hemisphere? *Radiocarbon* **55**, 2029–2034 (2013).
48. Faria, F. A., Albertoni, E. F. & Bugoni, L. Trophic niches and feeding relationships of shorebirds in southern Brazil. *Aquat. Ecol.* **52**, 281–296 (2018).
49. Bond, A. L. & Hobson, K. A. Reporting stable-isotope ratios in ecology: recommended terminology, guidelines and best practices. *Waterbirds* **35**, 324–331 (2012).
50. Parnell, A. C. et al. Bayesian stable isotope mixing models. *Environmetrics* **24**, 387–399 (2013).
51. Bergamino, L. et al. Autochthonous organic carbon contributions to the sedimentary pool: A multi-analytical approach in Laguna Garzón. *Org. Geochem.* **125**, 55–65 (2018).
52. Craven, K. F., Edwards, R. J. & Flood, R. P. Source organic matter analysis of saltmarsh sediments using SIAR and its application in relative sea-level studies in regions of  $\text{C}_4$  plant invasion. *Boreas* **46**, 642–654 (2017).
53. Lu, L. et al. Identifying organic matter sources using isotopic ratios in a watershed impacted by intensive agricultural activities in Northeast China. *Agric. Ecosyst. Environ.* **222**, 48–59 (2016).
54. Andrews, J. E., Greenaway, A. M. & Dennis, P. F. Combined carbon isotope and C/N ratios as indicators of source and fate of organic matter in a poorly flushed, tropical estuary: Hunts Bay, Kingston Harbour, Jamaica. *Estuar. Coast. Shelf Sci.* **46**, 743–756 (1998).
55. Lee, Y. I. L., Lim, H. S. & Yoon, H. I. L. Carbon and nitrogen isotope composition of vegetation on King George Island, maritime Antarctic. *Polar Biol.* **32**, 1607–1615 (2009).
56. Vega-García, S., Sánchez-García, L., Prieto-Ballesteros, O. & Carrizo, D. Molecular and isotopic biogeochemistry on recently-formed soils on King George Island (Maritime Antarctica) after glacier retreat upon warming climate. *Sci. Total Environ.* **755**, 142662 (2021).
57. Venturini, N., Cerpa, C., Moroni, L., Muniz, P., Kandratavicius, N., Rodríguez, M., Indacochea Mejía, A. C. Condor-Luján, B., Figueira, R.C.L. Biogeochemistry of surface sediments in an Antarctic nearshore area affected by recent glacier retreat: Collins Harbour, King George Island. SCAR Open Science Conference: Antarctic Science-Global Connections. Full Abstract Book (2020).
58. Martínez de la Escalera, G., Kruk, C., Segura, A. M. & Piccini, C. Effect of hydrological modification on the potential toxicity of *Microcystis aeruginosa* complex in Salto Grande reservoir, Uruguay. *Harmful Algae* **123**, 102403 (2023).
59. Callahan, B. J., McMurdie, P. J. & Holmes, S. P. Exact sequence variants should replace operational taxonomic units in marker-gene data analysis. *ISME J.* **11**, 2639–2643 (2017).
60. Callahan, B. J. et al. DADA2: High-resolution sample inference from Illumina amplicon data. *Nat. Methods* **13**, 581–583 (2016).
61. Quast, C. et al. The SILVA ribosomal RNA gene database project: improved data processing and web-based tools. *Nucleic Acids Res.* **41**, D590–D596 (2012).
62. Oberg, A. L. & Mahoney, D. W. Linear mixed effects models. In *Methods in Molecular Biology book series* (MIMB, volume 404), *Top. Biostat.* 213–234 (2007).
63. Oksanen, J.; Blanchet, F.G.; Friendly, M.; Kindt, R.; Legendre, P.; McGlinn, D.; Minchin, P.R.; O'Hara, R.B.; Simpson, G.L.; Solymos, P.; et al. Package 'Vegan'. Community Ecology Package, Version 2.5-7 (2019). Available online: <https://github.com/vegandevs/vegan> (Accessed on July 8, 2021).
64. Baselga, A. Partitioning the turnover and nestedness components of beta diversity. *Glob. Ecol. Biogeogr.* **19**, 134–143 (2010).
65. Baselga, A. & Orme, C. D. L. Betapart: An R package for the study of beta diversity. *Methods. Ecol. Evol.* **3**, 808–812 (2012).
66. Hammer, Ø., Harper, D. & Ryan, P. Past: Paleontological statistics software package for education and data analysis. *Paleontol. Electron.* **4**, 1–9 (2001).
67. Dufrière, M. & Legendre, P. Species assemblages and indicator species: the need for a flexible asymmetrical approach. *Ecol. Monogr.* **67**, 345–366 (1997).
68. Vera, E. I. & Cesari, S. N. Helechos arborescentes en la Antártida. CONICET Digit. **26**, 49–3 (2017).

## Acknowledgements

We thank all staff members from the Artigas Field Station (BCAA), the expeditions Antarkos XXXIV and XXXV and specially to J. Fonseca, C. Paolino, C. Bueno, P. Rodriguez and J. Gonzalez. Field work was funded by the Instituto Antártico Uruguayo (IAU), PEDECIBA-Geociencias and SNI-ANII. We also thank to the University of Innsbruck and the Austrian Science Fund for financial support (FWF project I-5824) to RS; and to CSIC project Grupos 2022 ID 128 for financial aid. LB is a research fellow of CNPq (310145/2022-8).

## Author contributions

CP.: performed the field work; opening of the core; obtaining of samples and DNA extraction; designed the figures and tables; participated in the interpretation of the results; wrote the original draft. FB.: performed the sequence analyses; participated in the interpretation of the results; R.S.: participated in the interpretation of the results; wrote the original draft. G.M.E., opening of the core and samples handling. L.P.: performed the age model; participated in the interpretation of the results. L.Bu.: stable isotopes determination and analysis; L. Ber.: stable isotopes analysis and estimations of organic matter origin; design of figures. H.E.: chronology model. F.G.R. conceived and supervised the study; performed the field work; opening of the core; obtaining samples and DNA extraction; wrote original draft. All authors contributed to finalize the manuscript.

## Competing interests

The authors declare no competing interests.

## Additional information

**Supplementary information** The online version contains supplementary material available at <https://doi.org/10.1038/s43247-024-01245-6>.

**Correspondence** and requests for materials should be addressed to C. Piccini.

**Peer review information** *Communications Earth and Environment* thanks Matej Roman and the other, anonymous, reviewer(s) for their contribution to the peer review of this work. Primary Handling Editors: Ola Kwiecień and Aliénor Lavergne. A peer review file is available.

**Reprints and permissions information** is available at <http://www.nature.com/reprints>

**Publisher's note** Springer Nature remains neutral with regard to jurisdictional claims in published maps and institutional affiliations.

**Open Access** This article is licensed under a Creative Commons Attribution 4.0 International License, which permits use, sharing, adaptation, distribution and reproduction in any medium or format, as long as you give appropriate credit to the original author(s) and the source, provide a link to the Creative Commons license, and indicate if changes were made. The images or other third party material in this article are included in the article's Creative Commons license, unless indicated otherwise in a credit line to the material. If material is not included in the article's Creative Commons license and your intended use is not permitted by statutory regulation or exceeds the permitted use, you will need to obtain permission directly from the copyright holder. To view a copy of this license, visit <http://creativecommons.org/licenses/by/4.0/>.

© The Author(s) 2024